Molecular Crystals and Liquid Crystals
Publication details, including instructions for authors and subscription information:
http://www.tandfonline.com/loi/gmcl16

# Perturbation Theory for Nematic Liquid Crystals of Axially Symmetric Molecules: II. Effect of Quadrupolar Forces

S. Singh [a b] & K. Singh [a]

[a] Department of Physics, Banaras Hindu University, Varanasi, 221005, INDIA

[b] Department of Physics, University of Guelph, Guelph, Ontario, NIG 2W1, Canada

Version of record first published: 20 Apr 2011.

To cite this article: S. Singh & K. Singh (1983): Perturbation Theory for Nematic Liquid Crystals of Axially Symmetric Molecules: II. Effect of Quadrupolar Forces, Molecular Crystals and Liquid Crystals, 101:1-2, 77-102

To link to this article: http://dx.doi.org/10.1080/00268948308072484

*Mol. Cryst. Liq. Cryst.*, 1983, Vol. 101, pp. 77–102
0026-8941/83/1012-0077/$18.50/0

Printed in the United States of America



# Perturbation Theory for Nematic Liquid Crystals of Axially Symmetric Molecules: II. Effect of Quadrupolar Forces

S. SINGH† and K. SINGH

*Department of Physics, Banaras Hindu University, Varanasi-221005, INDIA*

(*Received April 8, 1983*)

A statistical mechanical perturbation theory, that derives from the work of Singh and Singh, is applied to analyse the influence of quadrupole interaction on a variety of thermodynamic properties of nematic liquid crystals. Numerical evaluations are done for a model system in which molecules are assumed to interact via a pair potential having both repulsive and attractive parts. The repulsive interaction is represented by a repulsion between hard spherocylinders. The attractive potential, a function of only the centre of mass distance and the relative orientation between the two molecules, is represented approximately by the isotropic dispersion and anisotropic quadrupole interaction between two asymmetric molecules. The properties of the reference system and the first order perturbation term are calculated by assuming that an angle-dependent range parameter scales the pair correlation function such that it decouples the orientational degrees of freedom from the translational one. The functional form and the density dependence of the effective one-body orientational potential is discussed. It is found that the thermodynamic properties for the nematic–isotropic transition are highly sensitive to the form of effective one-body orientational potential. The influence of pressure on the stability, ordering and thermodynamic functions for the NI transition is analysed and found to be in accordance with the experimental observation.

## 1. INTRODUCTION

The stability of a nematic liquid crystal results from the forces between the constituent molecules. Since these molecules possess

†Present Address: Department of Physics, University of Guelph, Guelph, Ontario N1G 2W1, Canada.

strong anisotropy in both intermolecular repulsions and attractions, in the construction of a molecular theory for nematic liquid crystals, one faces the complication of dealing with both spatial and angular variables of the molecules which makes the task extremely difficult.

There have been a number of attempts,[1-4] in the past, to study the nematic–isotropic (NI) phase transition in liquid crystals by incorporating both anisotropic intermolecular repulsions and attractions in their models. Some of these theories are successful in predicting certain thermodynamic properties of common nematogens, for example, phase diagrams of homologous series, qualitative correct temperature dependence of long-range order parameter, etc., but very poor in predicting volume changes at transitions, latent heats, maximum supercooling temperatures, etc. The reason for at least some of their shortcomings is quite obvious. As none of them take full account of the orientational and spatial correlations between particles and treat both attractive and repulsive branches of intermolecular interactions accurately, they cannot be expected to be quantitative.

In a recent publication, Singh and Singh[5] (referred to as I hereafter) have developed a statistical mechanical perturbation theory to describe the equilibrium properties of nematic liquid crystals. In this theory the reference potential function is nonspherical and consists of the short-range rapidly varying repulsive part of the pair potential. The important factor is the recognition that the structure of the system (spatial and angular pair correlations) is primarily controlled by the short-ranged and harshly repulsive part of the pair potential. The thermodynamic properties were calculated for a trial system in which molecules were assumed to interact via a pair potential which has the repulsive part represented by a repulsion between hard spherocylinders and an attractive part which is the function of only the centre of mass distance and the relative orientation between the two molecules and represents approximately the interaction arising from dispersion interaction between two asymmetric molecules. The relative influence of length-to-width ratio of the molecular hard core and the anisotropy in their correlation function on the NI transition properties was investigated. It was found that the effects of spatial and orientational pair correlations on the thermodynamic properties are quite large and the properties are extremely sensitive to the values of molecular parameters.

In I by attributing the stabilizing nematic potential to anisotropic dispersion forces, the role of electrostatic interactions in determining the properties of liquid crystals has been largely neglected by Singh and Singh. The vast majority of nematic liquid crystals are polar but

the absence of ferroelectricity in them shows that there is equal probability of the dipole pointing in either direction. Because of this it is generally assumed that the dipolar interactions are only of marginal importance in stabilizing the nematic phase. However, there is some structural evidence,[6,7] from X-ray diffraction, that in the nematic phase of some strongly polar mesogens there exists considerable anti-parallel ordering of the molecules to which the dipolar interaction must contribute. The roles of dipoles in determining the properties of liquid crystals has been studied by Madhusudana and Chandrasekhar,[8] who found that the inclusion of short range dipole–dipole interaction raises the order parameter. Using the Maier and Meier theory[9] for taking account of antiferroelectric ordering they have also predicted a small incremental change in the mean permittivity at the NI transition. Since all the nematogens are strongly quadrupolar compounds it is useful and interesting to study the effects of quadrupole–quadrupole interaction on the thermodynamic properties of the NI phase transition.

In this paper we apply the perturbation theory of I to the computation of equilibrium properties of nematic liquid crystals by considering a model which takes into account the influence of quadrupolar forces and is at the same time consistent with the nonpolar character of the medium. A brief account of the perturbation expansion method and the working equations are given in Sec. 2. Results and discussions are presented in Sec. 3. In the last section the theory has been applied to analyse the thermodynamic data as obtained from the measurements under high pressure.

## 2. THEORY AND DERIVATION OF WORKING EQUATIONS

We consider a system of $N$ axially symmetric nonspherical nematogenic molecules contained in a volume $V$ at temperature $T$. The total potential energy of interaction of this system is approximated as the sum of the interaction energies of pairs. Thus,

$$U_N(\bar{X}_1, \ldots, \bar{X}_N) = \sum_{1 \le i < j \le N} u(\bar{X}_i, \bar{X}_j) \tag{1}$$

where the vector $\bar{X}_i = (\bar{r}_i, \Omega_i)$ represents both the position of the centre of mass and orientation of the $i$th molecule. The pair potential energy is written as a sum of two parts—one part of this division is known as reference potential $u_0$ and the other as perturbation poten-

tial $u_p$, i.e.

$$u(\bar{X}_i, \bar{X}_j) = u_0(\bar{X}_i, \bar{X}_j) + u_p(\bar{X}_i, \bar{X}_j) \tag{2}$$

The reference potential $u_0$ is chosen to include the rapidly varying short range repulsive part of the interaction whereas the perturbation potential $u_p$ contains the more smoothly varying long-range attractive part.

A perturbation calculation generally proceeds in two steps. The first task is to calculate the effect of the perturbation on the thermodynamic properties and pair distribution function of the reference system. The second step is to find a recipe to relate the properties of reference system to that of a system the properties of which are already known to a high degree of accuracy. A useful theory is one which converges rapidly.

Following the statistical mechanical machinery as outlined in I, we write the perturbation series for the Helmholtz free-energy as

$$\frac{\beta A}{N} = \frac{\beta A_0}{N} + \sum_{r=1}^{\infty} \frac{\beta A^{(r)}}{N} \tag{3}$$

where $A_0$ is the reference system contribution to $A$ and

$$\frac{\beta A^{(r)}}{N} = \beta \int f(\Omega_p)\, d\Omega_p\, \Psi^{(r)}(\Omega_p) \tag{4}$$

represents the perturbation terms, $r$ denotes the order of perturbation and $\psi(\Omega_p)$ is defined as effective one-body orientational perturbation potential by the relation

$$\psi^{(r)}(\Omega_p) = \tfrac{1}{2} r\rho \int d\Omega_{p'} f(\Omega_{p'}) \int d\bar{r}\, u_p(\bar{r}, \Omega_p, \Omega_{p'})\, g^{(r-1)}(\bar{r}, \Omega_p, \Omega_{p'}) \tag{5}$$

The zeroth order terms refer to quantities corresponding to the reference system and all the other symbols have their usual meaning.[5]

As discussed in detail in I for applying the perturbation theory, we write Eq. (2) in the following form:

$$u(\bar{r}_{12}, \Omega_1, \Omega_2) = u_{hr}(\bar{r}_{12}, \Omega_1, \Omega_2) + u_p(\bar{r}_{12}, \Omega_1, \Omega_2) \tag{6}$$

where $u_{hr}(\bar{r}_{12}, \Omega_1, \Omega_2)$ represents the repulsion between hard spherocylinders of length $2b$ and diameter $2a$ (the length to width ratio $x = 2b/2a$). $u_{hr}(\bar{r}_{12}, \Omega_1, \Omega_2) = \infty$, for any $r_{12}, \Omega_1, \Omega_2$ such that the rods 1 and 2 overlap and equal to zero otherwise. The following form for the perturbation potential was adopted in I

$$u_p(\bar{r}_{12}, \Omega_1, \Omega_2) = -r_{12}^{-6}(C_i + C_a P_2(\cos\theta_{12})), \quad \text{for } r_{12} > D(\Omega_1, \Omega_2) \tag{7}$$

where $C_i$ and $C_a$ are the constants related with the isotropic and anisotropic dispersion interactions and $\theta_{12}$ is the angle between the orientations of the two molecules. $D(\Omega_1, \Omega_2)$ represents the value of the distance of closest approach between the two interacting molecules.

In the present calculation we approximate the perturbation potential by the relation,

$$u_p(\bar{r}_{12}, \Omega_1, \Omega_2) = -\frac{C_i}{r_{12}^6} - \frac{C_a}{r_{12}^5} P_2(\cos\theta_{12}), \quad \text{for } r_{12} > D(\Omega_1, \Omega_2) \tag{8}$$

where the first term represents the isotropic component of dispersion interaction and the second one the quadrupole–quadrupole interaction. $C_i$ and $C_a$ are the constants related with the respective interactions. There are two reasons for our choice of such a simple trial potential. First, such a pair potential is in accord with the Maier-Saupe theory, and so enables us to test the molecular field approximation employed in the theory when there is translational disorder. Secondly, it provides a convenient means to study the effects of quadrupole interaction and the coupling between isotropic dispersion and anisotropic quadrupole interactions on the thermodynamic properties of nematic liquid crystals.

### 2.1. Thermodynamics of reference system

In order to calculate the thermodynamic properties of a system of hard spherocylinders interacting via the pair potential $u_0(\bar{r}_{12}, \Omega_{12})$ which satisfies the relation

$$\begin{aligned} u_0(\bar{r}_{12}, \Omega_{12}) &= u_0[r_{12}/D(\Omega_{12})] \\ &= u_0(r_{12}^*) = \begin{cases} \infty & \text{for} \quad r_{12}^* < 1 \\ 0 & \text{for} \quad r_{12}^* > 1 \end{cases} \end{aligned} \tag{9}$$

where $D(\Omega_{12})$ is the distance of closest approach of two molecules having relative orientation $\Omega_{12}$, we start with the pressure equation

$$\frac{\beta p_0}{\rho} = 1 - \frac{1}{6}\beta\rho \int d\bar{r} f(\Omega_1)\, d\Omega_1 \int f(\Omega_2)\, d\Omega_2 \times \left[r \nabla u_0(\bar{r}_{12}, \Omega_{12})\right] g^{(0)}(\bar{r}_{12}, \Omega_{12}) \tag{10}$$

in which the operator $\nabla$ acts on the $\bar{r}_{12}$ coordinates of $u_0(\bar{r}_{12}, \Omega_{12})$. Using the decoupling approximation[10]

$$g^{(0)}(\bar{r}_{12}, \Omega_{12}) = g^{(0)}\left[r_{12}/D(\Omega_{12})\right] = g^{(0)}\left(r_{12}^*\right) \tag{11}$$

which completely decouples the orientational and positional degrees of freedom, we get

$$\frac{\beta p_0}{\rho} = 1 + \frac{1}{2}\rho g_{\mathrm{HS}}(1) \int f(\Omega_1)\, d\Omega_1 \int f(\Omega_2)\, d\Omega_2\, V_{\mathrm{exc}}(\Omega_{12}) \tag{12}$$

where $V_{\mathrm{exc}}(\Omega_{12})$ is the excluded volume, or co-volume, between the two rods,

$$V_{\mathrm{exc}}(\Omega_{12}) = \frac{1}{3}\int D^3(\Omega_{12})\, d\bar{r}_{12} = 8V_0(1 - \chi^2)^{-1/2}(1 - \chi^2\cos^2\theta_{12})^{1/2} \tag{13}$$

$g_{\mathrm{HS}}(1)$ is the value of the radial distribution of hard sphere at core, $V_0$ the volume of a molecule and

$$\chi = \frac{x^2 - 1}{x^2 + 1} \tag{14}$$

with $x$ as length-to-width ratio of a hard spherocylinder. Eq. (13) now reduces to

$$\frac{\beta p_0}{\rho} = 1 + \frac{2\eta(2 - \eta)}{(1 - \eta)^3}\left[F_1(\chi) - F_2(\chi)S^2\right] \tag{15}$$

where

$$\eta = \rho V_0; \qquad F_1(\chi) = (1 - \chi^2)^{-1/2}\left(1 - \tfrac{1}{6}\chi^2 - \tfrac{1}{40}\chi^4 - \tfrac{1}{112}\chi^6 - \cdots\right) \tag{16}$$

and

$$F_2(\chi) = \tfrac{1}{3}\chi^2(1-\chi^2)^{-1/2}\left[1 + \tfrac{3}{14}\chi^2 + \tfrac{5}{64}\chi^4 + \cdots\right] \quad (17)$$

The Helmholtz free energy per particle for the reference system can now be evaluated from Eq. (15) by using the standard thermodynamic relation and finally we get,

$$\frac{\beta A_0}{N} = (\ln\rho - 1) + \langle \ln[4\pi f(\Omega)]\rangle + \frac{\eta(4-3\eta)}{(1-\eta)^2}\left[F_1(\chi) - F_2(\chi)S^2\right] \quad (18)$$

where the first two terms represent the free-energy of a gas of noninteracting rods and the last term is the excess free energy which arises due to the inter-particle interaction. The angular bracket $\langle\text{—}\rangle$ denotes the ensemble average over the N–1 particles of the system.

Other thermodynamic properties of the reference system can be evaluated by using Eqs. (15) and (18) and the standard thermodynamic relations.

### 2.2. Thermodynamics of the first-order perturbation term

The Helmholtz free-energy in the first-order perturbation is

$$\frac{\beta A^{(1)}}{N} = \beta \int d\Omega_1 f(\Omega_1)\psi^{(1)}(\Omega) \quad (19)$$

where $\psi^{(1)}(\Omega)$ is given by

$$\psi^{(1)}(\Omega) = \tfrac{1}{2}\rho \int d\Omega_2 f(\Omega_2) \int d\bar{r}\, u_p(\bar{r}, \Omega_1, \Omega_2) g^{(0)}(\bar{r}, \Omega_1, \Omega_2) \quad (20)$$

In the assumed trial system, the first-order perturbation term, as obvious, involves the hard spherocylinder's pair correlation function (PCF) $g^{(0)}(\bar{r}, \Omega_1, \Omega_2)$. The PCF is related to the probability of finding a hard spherocylinder with known orientation at a given distance from the reference hard spherocylinder whose position and orientation are known. In general, a detailed knowledge of the PCF as a function of $\bar{r}$, $\Omega_1$, and $\Omega_2$ (in total five scalars $r$, $\bar{r}\cdot\Omega_1$, $\bar{r}\cdot\Omega_2$, $\Omega_1\cdot\Omega_2$ and $\Omega_1\times\Omega_2\cdot\bar{r}$) is needed in the evaluation of perturbation terms. However, in our present development we need to know only $g^{(0)}(r, \Omega_{12})$ which is

defined as

$$g^{(0)}(r, \Omega_{12}) = \int d\hat{r}\, g^{(0)}(\bar{r}, \Omega_1, \Omega_2) \tag{21}$$

where $\hat{r}$ is a unit vector along the axis joining the centres of the two spherocylinders. The integration in Eq. (21) is performed by keeping the relative orientation $\Omega_{12}$ between two molecules fixed. Unfortunately, we know little about $g^{(0)}(\bar{r}, \Omega_1, \Omega_2)$ and, therefore about $g^{(0)}(r, \Omega_{12})$. We evaluate the first-order perturbation term by assuming that the reference system PCF can be approximated by Eq. (11). Let

$$Y(\Omega_{12}) = -\int dr^3 \left[\frac{C_i}{r^6} + \frac{C_a}{r^5} P_2(\cos\theta_{12})\right] g^{(0)}(r, \Omega_{12}) \tag{22}$$

Reducing the distance variables with $D(\Omega_{12})$, we get

$$Y(\Omega_{12}) = -C_i I_6(\rho, T) I_6(\theta_{12}) - C_a P_2(\cos\theta_{12}) I_5(\rho, T) I_5(\theta_{12}) \tag{23}$$

where

$$I_n(\rho, T) = \int_0^\infty dr^* r^{*2-n} g_{HS}^{(0)}(r^*) \tag{24}$$

$$I_n(\theta_{12}) = \int \frac{d\hat{r}}{D^{n-3}(\Omega_{12})} \tag{25}$$

Taking the Berne and Puchukas[11] expression for $D(\hat{r}, \Omega_{12})$,

$$D(\hat{r}, \Omega_{12}) = D_0 \left[1 - \chi \frac{(\hat{r}\cdot\hat{e}_1)^2 + (\hat{r}\cdot\hat{e}_2)^2 - 2\chi(\hat{r}\cdot\hat{e}_1)(\hat{r}\cdot\hat{e}_2)(\hat{e}_1\cdot\hat{e}_2)}{1 - \chi^2(\hat{e}_1\cdot\hat{e}_2)^2}\right]^{-1/2} \tag{26}$$

where $\hat{e}_1$ and $\hat{e}_2$ are the unit vectors along the symmetry axes of two interacting spheroids and $D_0 = 2a$, the integral (25) for $n = 6$ and 5 have been evaluated for fixed orientation $\hat{e}_1 \cdot \hat{e}_2 = \cos\theta_{12}$. For convenience we write our result as an expansion in the Legendre functions

$$I_n(\theta_{12}) = \frac{1}{D_0^{n-3}}\left[A_0^{(n)} + A_2^{(n)} P_2(\cos\theta_{12}) + A_4^{(n)} P_4(\cos\theta_{12}) + A_6^{(n)} P_6(\cos\theta_{12}) + \cdots\right] \tag{27}$$

We evaluate the values of the constants $A_m^{(n)}$ as a function of length to width ratio $x$. Table I reports the values of the constants $A_m^{(5)}$ related with the integral $I_5(\theta_{12})$. For the corresponding values of the constants $A_m^{(6)}$ of the integral $I_6(\theta_{12})$ we refer to $I$. Using the exact radial distribution function for hard spheres obtained from computer simulation the integral (24) can be evaluated to yield the values of $I_n(\rho, T)$. Combining the known density expansion for $g_{HS}^{(0)}(r^*)$ with the Monte-Carlo values, Larsen *et al.*[12] have found the following extended series

$$I_n(\rho^*) = J_{0,n} + J_{1,n}\rho^* + J_{2,n}\rho^{*2} + J_{3,n}\rho^{*3} + J_{4,n}\rho^{*4} + J_{5,n}\rho^{*5} \tag{28}$$

where

$$\rho^* = \frac{6}{\pi}\rho V_0$$

The coefficients $J_{m,n}$'s are tabulated by Larsen *et al.*[12] for several values of $n$ ($= 0$ to 24).

TABLE I

The values of the constants of Eq. (27) for the potential model of Eq. (8) as a function of the length to width ratio $x$

| $x$ | $A_0^{(5)}$ | $A_2^{(5)}$ | $A_4^{(5)}$ | $A_6^{(5)}$ | $A_8^{(5)}$ | $A_{10}^{(5)}$ | $A_{12}^{(5)}$ |
|---|---|---|---|---|---|---|---|
| 1.5 | 9.623697 | 0.581983 | 0.03196005 | 0.001550 | 0.000071 | 0.000003 | 0.0000001 |
| 2.0 | 8.060054 | 1.160006 | 0.17731524 | 0.023915 | 0.003054 | 0.000384 | 0.000049 |
| 2.5 | 7.113094 | 1.4603489 | 0.3698605 | 0.082543 | 0.01741343 | 0.0037288 | 0.000798 |
| 3.0 | 6.489715 | 1.5767060 | 0.5447906 | 0.1656061 | 0.047528 | 0.0144259 | 0.004229 |
| 3.5 | 6.054573 | 1.590725 | 0.6800269 | 0.2553117 | 0.0905037 | 0.0355452 | 0.0128372 |
| 4.0 | 5.737244 | 1.551129 | 0.7749324 | 0.3394401 | 0.1406589 | 0.0676894 | 0.02828549 |
| 4.5 | 5.4978174 | 1.485090 | 0.8360080 | 0.41204789 | 0.1928994 | 0.1096300 | 0.0509409 |
| 5.0 | 5.312168 | 1.407540 | 0.87091297 | 0.4713813 | 0.243754 | 0.1592507 | 0.0801248 |
| 5.5 | 5.164955 | 1.326642 | 0.8864395 | 0.5179503 | 0.2912553 | 0.2142326 | 0.11457709 |
| 6.0 | 5.046020 | 1.2468132 | 0.8880419 | 0.5532760 | 0.334505 | 0.272433 | 0.15284604 |
| 6.5 | 4.948399 | 1.1703699 | 0.8799035 | 0.5791887 | 0.3732273 | 0.332051 | 0.1935373 |
| 7.0 | 4.887187 | 1.098144 | 0.8651549 | 0.5974737 | 0.40770113 | 0.3916658 | 0.2354398 |
| 7.5 | 4.798832 | 1.0314916 | 0.846102 | 0.60971812 | 0.43811987 | 0.4502139 | 0.27757074 |
| 8.0 | 4.740714 | 0.9695857 | 0.824422 | 0.6172621 | 0.4649334 | 0.5069388 | 0.31917397 |
| 8.5 | 4.690859 | 0.9125852 | 0.8013234 | 0.6212022 | 0.488558 | 0.561333 | 0.359695 |
| 9.0 | 4.647758 | 0.8602343 | 0.7776627 | 0.62241737 | 0.5093898 | 0.6130826 | 0.398749 |
| 9.5 | 4.610232 | 0.8122216 | 0.7540402 | 0.62160189 | 0.5277889 | 0.6620229 | 0.4360857 |
| 10.0 | 4.577360 | 0.7682155 | 0.7308664 | 0.6192985 | 0.5440750 | 0.7080968 | 0.4715589 |

With the help of Eqs. (23), (24) and (27), we express Eq. (20) in the following form:

$$\psi^{(1)}(\cos\theta_1) = -\phi_0 - \phi_2 S_2 P_2(\cos\theta_1) - \phi_4 S_4 P_4(\cos\theta_1) + \cdots \tag{29}$$

where

$$\phi_0 = \left(\frac{\pi x}{12}\right) C_i^* A_0^{(6)} \eta I_6(\eta) + \frac{1}{10}\left(\frac{\pi x}{6}\right)^{2/3} C_a^* A_2^{(5)} \eta I_5(\eta) \tag{30}$$

$$\phi_2 = \left(\frac{\pi x}{12}\right) C_i^* A_2^{(6)} \eta I_6(\eta) + \frac{1}{2}\left(\frac{\pi x}{6}\right)^{2/3} \times C_a^* \left[A_0^{(5)} + \frac{2}{7}\left(A_2^{(5)} + A_4^{(5)}\right)\right] \eta I_5(\eta) \tag{31}$$

$$\phi_4 = \left(\frac{\pi x}{12}\right) C_i^* A_4^{(6)} \eta I_6(\eta) + \frac{1}{2}\left(\frac{\pi x}{6}\right)^{2/3} \times C_a^* \left[\frac{18}{35} A_2^{(5)} + \frac{20}{77} A_4^{(5)}\right] \eta I_5(\eta) \tag{32}$$

$$S_n = \int f(\Omega_2)\, d\Omega_2\, P_n(\cos\theta_2) \tag{33}$$

and

$$C_i^* = C_i / V_0^2, \qquad C_a^* = C_a / V_0^{5/3}$$

The values of $\phi_0$, $\phi_2$ and $\phi_4$ are given in Table II for $x = 1.0$, 1.5, 2.0, 2.5 and 3.0. The variations of $\phi_2^*$ and $\phi_4^*$ as a function of $v^*$, where $\phi_n^* = \phi_n / C_i^*$ and $v^* = 1/\rho^*$, are shown in Figures 1 and 2 for several values of $x$. There are seen a linear volume dependence of $\phi_2$ and $\phi_4$.

We see from Table II that the average contribution of $\phi_2$ and $\phi_4$ increases with $x$. The contribution of $\phi_4$ is about 13% with respect to $\phi_2$ for $x = 2$ and about 30% for $x = 3$. Therefore the contribution of $\phi_4$ for $x \geq 2$ is substantial and cannot be neglected. However, in the present work we approximate the effective one-body orientational potential $\psi(\Omega)$ by the first two terms of Eq. (29),

$$\psi(\Omega) \simeq -\phi_0 - \phi_2 S P_2(\cos\theta_1) \tag{34}$$

Here and onward we drop the subscript 2 from $S_2$. Under this approximation, which is valid only for $x \leq 2$, the free energy is written as

$$\frac{\beta A^{(1)}}{N} = -\beta\phi_0 - \beta\phi_2 S^2 \tag{35}$$

TABLE II

The values of function $\phi_0^*$, $\phi_2^*$, $\phi_4^*$ and $\phi_4^*/\phi_2^*$ (as defined in Eq. (29)) as a function of packing fraction $\eta$ and length-to-width ratio $x$ for $C_i^*/C_a^* = 8$, $\phi_\eta^* = \phi_\eta/C_i^*$

| $x$ | $\eta$ | $\phi_0^*$ | $\phi_2^*$ | $\phi_4^*$ | $\phi_4^*/\phi_2^*$ |
|---|---|---|---|---|---|
| 1.0 | 0.3 | 0.47854 | 0.10147 | 0 | 0 |
| | 0.4 | 0.71810 | 0.14745 | 0 | 0 |
| | 0.5 | 1.00550 | 0.20000 | 0 | 0 |
| | 0.6 | 1.3434 | 0.259075 | 0 | 0 |
| | 0.7 | 1.73144 | 0.324119 | | |
| 1.5 | 0.3 | 0.48772 | 0.15026 | 0.00638 | 0.04246 |
| | 0.4 | 0.73181 | 0.22056 | 0.00942 | 0.042708 |
| | 0.5 | 1.0246 | 0.30223 | 0.01298 | 0.042955 |
| | 0.6 | 1.36890 | 0.39548 | 0.01708 | 0.043198 |
| | 0.7 | 1.764116 | 0.499705 | 0.02170 | 0.043435 |
| 2.0 | 0.3 | 0.51102 | 0.21929 | 0.02877 | 0.131195 |
| | 0.4 | 0.76669 | 0.32393 | 0.04278 | 0.1320676 |
| | 0.5 | 1.07335 | 0.44669 | 0.05938 | 0.1329309 |
| | 0.6 | 1.43387 | 0.588129 | 0.07867 | 0.1337708 |
| | 0.7 | 1.84767 | 0.74755 | 0.10060 | 0.13457 |
| 2.5 | 0.3 | 0.542478 | 0.272927 | 0.059257 | 0.21632 |
| | 0.4 | 0.813874 | 0.405730 | 0.088437 | 0.217968 |
| | 0.5 | 1.139397 | 0.560969 | 0.123182 | 0.219589 |
| | 0.6 | 1.522077 | 0.740490 | 0.163764 | 0.221157 |
| | 0.7 | 1.9613218 | 0.943523 | 0.210078 | 0.22265 |
| 3.0 | 0.3 | 0.58178 | 0.31660 | 0.97037 | 0.30649 |
| | 0.4 | 0.87276 | 0.46944 | 0.14485 | 0.30857 |
| | 0.5 | 0.122173 | 0.64973 | 0.201811 | 0.31061 |
| | 0.6 | 1.63194 | 0.85853 | 0.26835 | 0.31257 |
| | 0.7 | 2.102726 | 1.094987 | 0.34431 | 0.31445 |

The first-order perturbation contribution to the compressibility factor is given by

$$\frac{\beta p^{(1)}}{\rho} = -\left(\frac{\pi x}{12}\right)\frac{C_i^*}{k}\left(A_0^{(6)} + A_2^{(6)}S^2\right)\left[I_6(\eta) + \eta\frac{\partial I_6(\eta)}{\partial \eta}\right]\frac{\eta}{T}$$
$$-\frac{1}{2}\left(\frac{\pi x}{6}\right)^{2/3}\frac{C_a^*}{k}\left(\frac{1}{5}A_2^{(5)} + \left[A_0^{(5)} + \frac{2}{7}\left(A_2^{(5)} + A_4^{(5)}\right)\right]S^2\right)$$
$$\times\left[I_5(\eta) + \eta\frac{\partial I_5(\eta)}{\partial \eta}\right]\frac{\eta}{T} \qquad (36)$$

Expressions for the other thermodynamic properties can be derived using the Eqs. (35), (36) and standard thermodynamic relations.

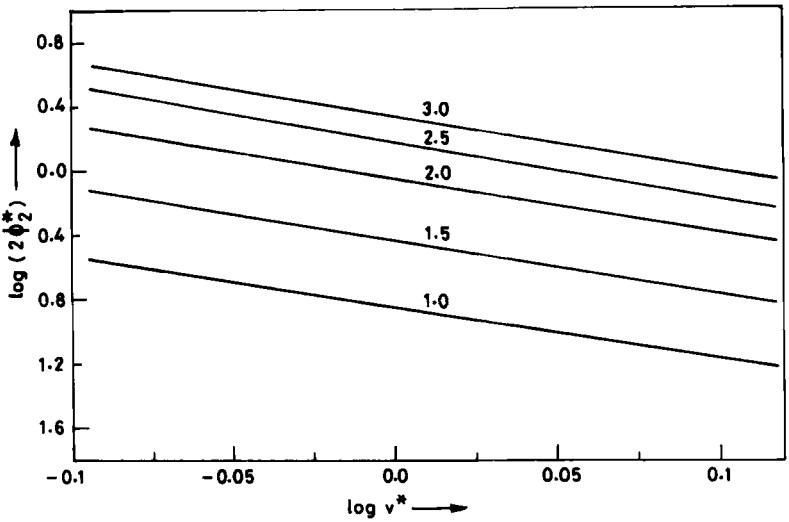


FIGURE 1 The volume dependence of the interaction parameter $\phi_2^*$ for effective one-body orientational parameter for $C_i^*/C_a^* = 8$. The number on the curves indicates the value of $x$.

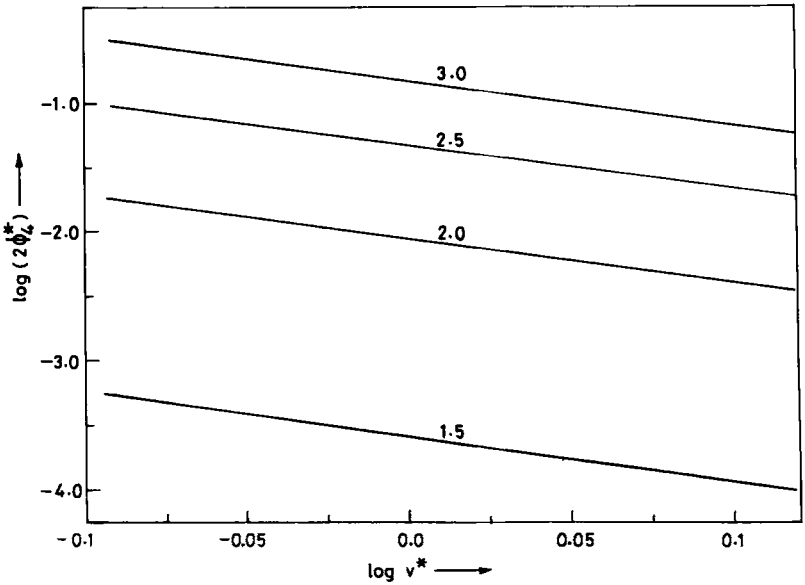


FIGURE 2 The volume dependence of the interaction parameter $\phi_4^*$ for effective one-body orientational parameter for $C_i^*/C_a^* = 8$. The number on the curves indicates the value of $x$.

### 2.3. Thermodynamic equilibrium

With the help of relations (18) and (35), the total configurational Helmholtz free-energy can be written as

$$\frac{\beta A}{N} = \langle \ln[4\pi f(\Omega)] \rangle + C_2 - B_2 S^2 \tag{37}$$

where

$$C_2 = \ln \rho - 1 + \frac{\eta(4 - 3\eta)}{(1 - \eta)^2} F_1(\chi) - \left(\frac{\pi x}{12}\right) \frac{C_i^*}{k} \left[ A_0^{(6)} I_6(\eta) + \frac{1}{5} \left(\frac{\pi x}{6}\right)^{-1/3} \frac{C_a^*}{C_i^*} A_2^{(5)} I_5(\eta) \right] \frac{\eta}{T} \tag{38}$$

and

$$B_2 = \frac{\eta(4 - 3\eta)}{(1 - \eta)^2} F_2(\chi) + \left(\frac{\pi x}{12}\right) \frac{C_i^*}{k} \times \left[ A_2^{(6)} I_6(\eta) + \left(\frac{\pi x}{6}\right)^{-1/3} \frac{C_a^*}{C_i^*} \left( A_0^{(5)} + \frac{2}{7} \left( A_2^{(5)} + A_4^{(5)} \right) \right) I_5(\eta) \right] \frac{\eta}{T} \tag{39}$$

The one-particle orientational distribution at a specified temperature and pressure is determined by minimizing the free-energy with respect to the variations of $f(\Omega)$ subject to constraint

$$\int f(\Omega)\, d\Omega = 1 \tag{40}$$

From Eqs. (37) and (40), $f(\Omega)$ can be written as

$$f(\Omega) = \frac{\exp[2 B_2 S P_2(\cos\theta)]}{\int \exp[2 B_2 S P_2(\cos\theta)]\, d\Omega} \tag{41}$$

which leads directly to a transcendental equation for the lowest-order parameter $S$ ($= \langle P_2(\cos\theta) \rangle$):

$$S = \frac{\int P_2(\cos\theta) \exp[2 B_2 S P_2(\cos\theta)]\, d\Omega}{\int \exp[2 B_2 S P_2(\cos\theta)]\, d\Omega} \tag{42}$$

For $B_2 > 2.27$ two solutions of the above Eq. (42) are obtained which correspond to local minima in the free-energy. One is associated with $S = 0$ and represents isotropic liquid. The other one with $S > 0$ corresponds to a nematic phase. A comparison of the values of free-energies associated with both the minima decides which solution is physically reliable.

The NI transition at constant pressure is located by equating the pressure and chemical potentials of the two phases,

$$P_{\text{nem}}(\eta_{nc}, T_c, S_c) = P_{\text{iso}}(\eta_{ic}, T_c)$$
$$\mu_{\text{nem}}(\eta_{nc}, T_c, S_c) = \mu_{\text{iso}}(\eta_{ic}, T_c) \tag{43}$$

$S_c$ is determined from Eq. (42). Keeping the pressure fixed, we get four equations involving four unknowns $\eta_{nc}$, $\eta_{ic}$, $T_c$ and $S_c$. These unknown parameters can, therefore, be determined by solving simultaneously Eqs. (42) and (43).

## 3. RESULTS AND DISCUSSION

### 3.1. Properties at the N–I phase transition

In this section, we first investigate the effect of the spherocylindrical hard-core length to width ratio $x$ and the potential parameters $C_i$ and $C_a$ as defined in Eq. (8) on the thermodynamic properties of NI phase transition. The results obtained here and in I (using potential of Eq. (7)) are compared.

The variation of packing fraction, order parameter and relative density change at the NI transition are shown in Figure 3. In this calculation the following values of the interaction parameters and the molecular volume have been used,

$$C_i^*/k = 4000 \text{ (K)}$$
$$C_a^*/C_i^* = 1/12 \quad \text{and} \quad 1/50$$

and

$$V_0 = 230 \text{ (Å}^3\text{)}$$

These values of the interaction parameters and $V_0$ have been chosen simply because they approximately correspond to the values used in the calculation of the NI transition of para-azoxyanisole (PAA) by

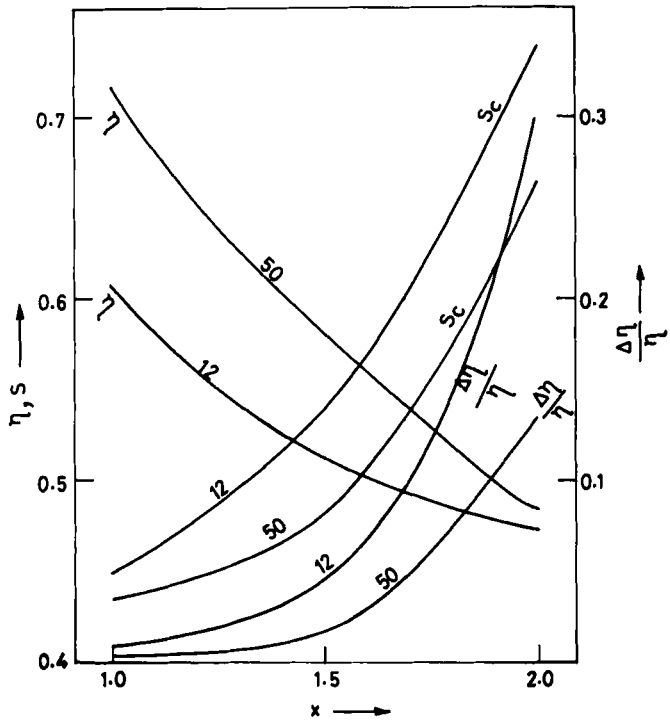


FIGURE 3 The variation of packing fraction $\eta$, order parameter $S_c$ and the relative density change $\Delta\eta/\eta$ at the nematic–isotropic transition as a function of $x$ for a given interaction strength $C_i^*/k = 4000$ (K). The number on the curves indicates the value of $C_i^*/C_a^*$ and the molecular volume $V_0 = 230$ Å$^3$.

several other workers. Figures 5 and 6 show, respectively, the variation of transition temperature $T_c$ with $C_i^*/k$ and $C_a^*/C_i^*$ for the different values of $x$. As obvious from these figures our calculation, as physically expected, predicts that as $x$ increases the phase transition is shifted to higher temperatures, lower density with increasing density change and jump of the order parameter. Further, the calculation shows that the interaction parameters $C_i$ and $C_a$ have a strong influence on the thermodynamic properties at the transition. Similar calculation is reported in I by assuming that the perturbation potential arises due to dispersion interaction Eq. (7). In Figures 4, 5 and 6 we have plotted, in fact, two sets of results as obtained in I and here for the pair potentials represented by Eqs. (7) and (8) which differ in the form adopted for the distance dependence of the anisotropic components. Although these results are found to be qualitatively similar, the

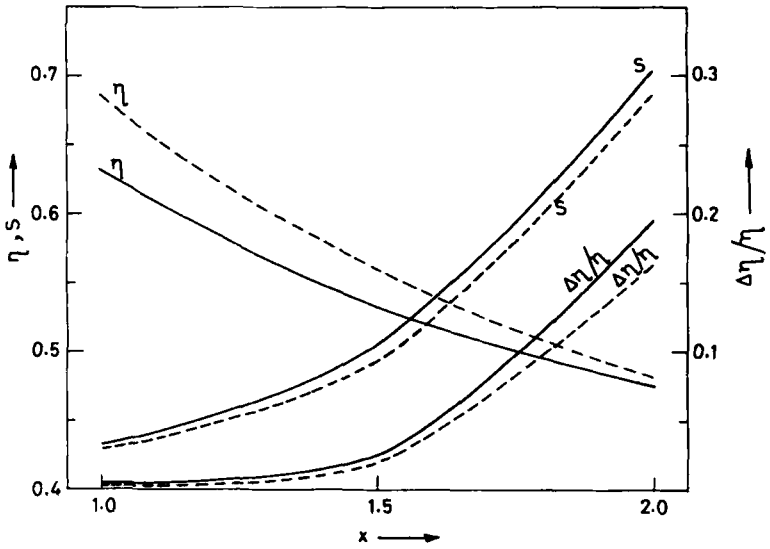


FIGURE 4 A comparison of the nematic–isotropic transition parameters as obtained in I (dashed line curves) and in the present work (solid line curves) for the potential parameters $C_i^*/k = 4000$ (K) and $C_i^*/C_a^* = 20$.

predicted NI transition is more pronounced in the case of anisotropic dispersion interaction.

Figure 8 shows the variation of order parameter $S$ as a function of $C_i^*/C_a^*$. For the packing fraction and the relative change in density a similar variation has been plotted in Figure 7. All the values of these figures correspond to the transition temperature $T_c \simeq 409$ K. Similar results obtained in I have also been plotted in these figures. We find that for a given value of $C_i^*$ as the ratio $C_i^*/C_a^*$ increases the relative change in the density at the transition decreases rapidly whereas the packing fraction $\eta$ increases slowly. At the higher values of $C_i^*/C_a^*$ ($> 20$) the calculated phase transition quantities are neither very sensitive to the values of $C_i^*/C_a^*$ nor to the potential model used.

A number of properties of the model system (Eq. (8)) at the NI transition temperature (with $pv_0/k = 1.69$ K) are summarized in Table III for the three values of $x$. For a given $x$ and $C_a^*/C_i^*$, the parameter $C_i^*/k$ was chosen so as to reproduce quantitatively the transition temperature $T_c \simeq 409$ K which, in fact, corresponds to the NI transition temperature of the most common nematogen PAA. The parameter $\Gamma$ given in the table measures the relative sensitivity of the order parameter to volume change (at constant

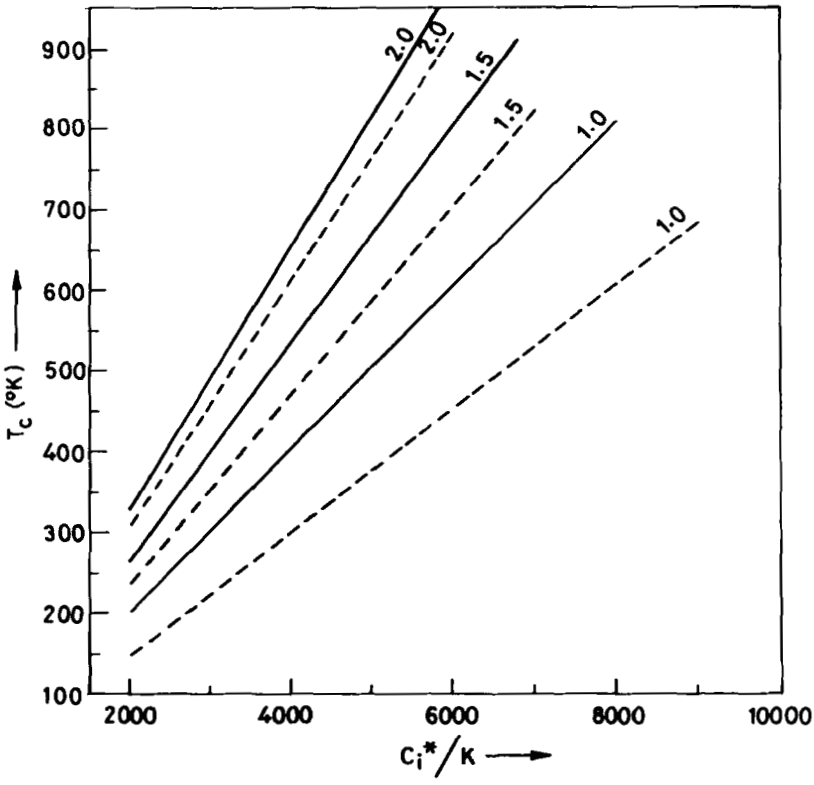


FIGURE 5 The variation of nematic–isotropic transition temperature $T_c$ as a function of $C_i^*/k$ for a fixed value of $C_i^*/C_a^* = 8$. The number on the curves indicates the value of $x$. The values as obtained in I and here are given, respectively, by the dashed and solid line curves.

temperature) and the temperature change (at constant volume) and is defined by the relation,

$$\Gamma = \frac{V}{T}\left(\frac{(\partial S/\partial T)_T}{(\partial S/\partial T)_V}\right) \equiv -\left(\frac{\partial \ln T}{\partial \ln V}\right)_S = \left(\frac{\partial \ln T}{\partial \ln \rho}\right)_S \cdots \quad (44)$$

The pressure dependence of the transition temperature ($dT_c/dp$) is determined by Clausius–Clapeyron's law. $\Delta\Sigma/Nk$ measures the change in entropies at the transition. Due to the choice of the trial potential model we expect that our results may not agree with the values for any real system. However, for the sake of comparison we also list in the

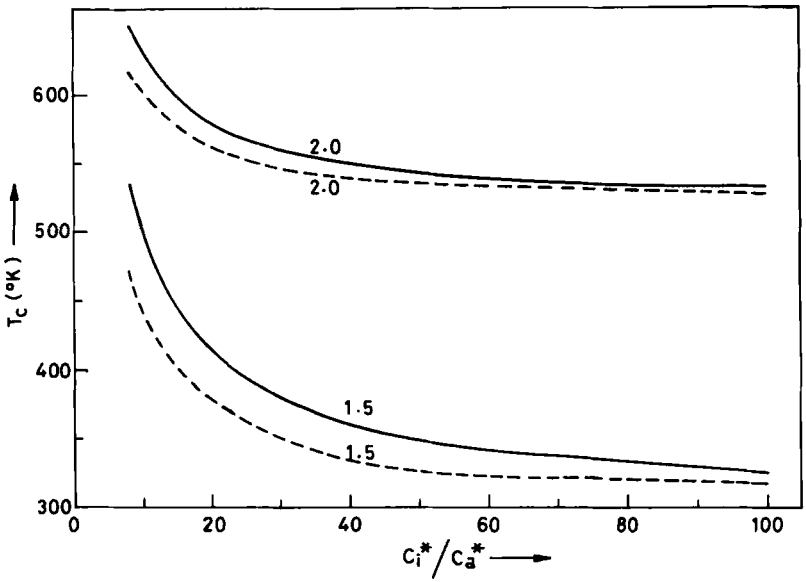


FIGURE 6 The variation of nematic–isotropic transition temperature $T_c$ as a function of $C_i^*/C_a^*$ for a fixed value of $C_i^*/k = 4000$ (K). The line symbols are the same as that of Figure 5.

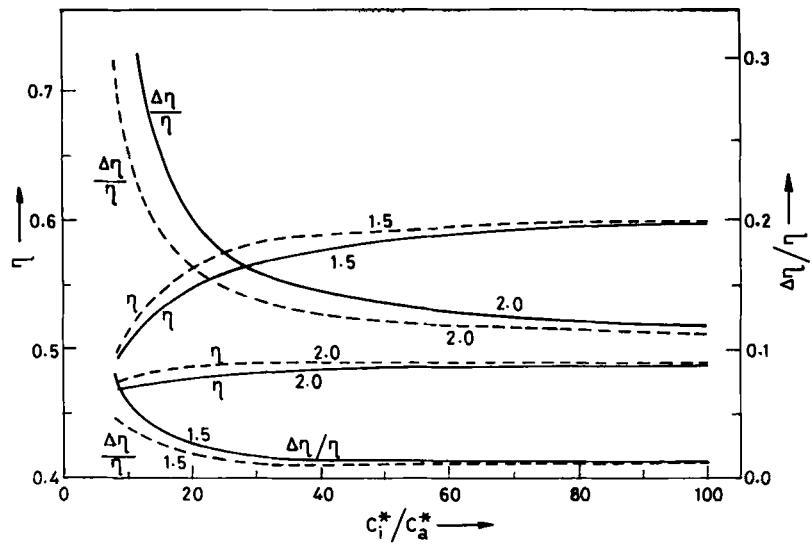


FIGURE 7 The variation of packing fraction $\eta$ and the relative change in density $\Delta\eta/\eta$ at the transition as a function of $C_i^*/C_a^*$. $C_i^*/k$ are chosen so as to reproduce the nematic–isotropic transition temperature $T_c \simeq 409$ (°K). The number on the curves indicates the value of $x$. The line symbols are the same as that of Figure 5.

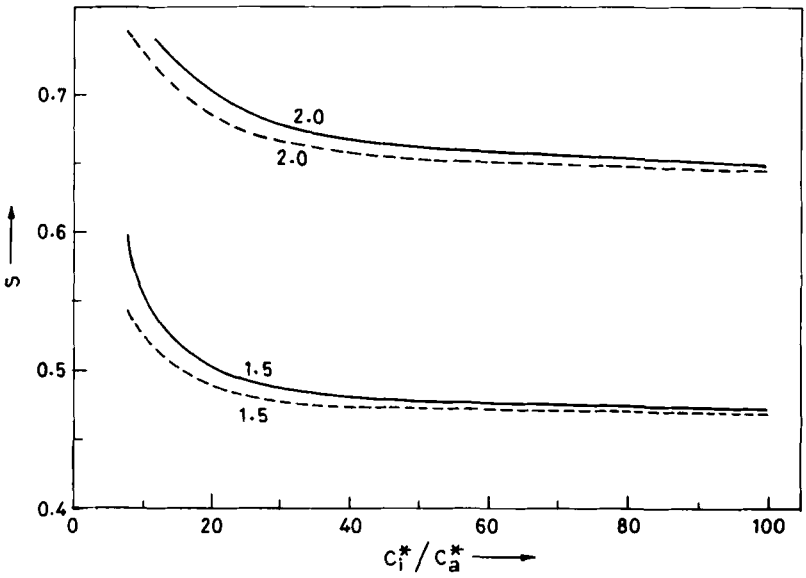


FIGURE 8 The variation of order parameter $S$ at the transition as a function of $C_i^*/C_a^*$. $C_i^*/k$ are chosen so as to reproduce the nematic–isotropic transition temperature $T_c \simeq 409$ (°K). The number on the curves indicates the value of $x$. The line symbols are the same as that of Figure 5.

table the experimental values of the transition properties for PAA and PAP.

Table IV compares the values of the NI transition properties as obtained in I and here using, respectively, the model potentials represented by Eqs. (7) and (8). It can be seen that for a given $x$ and $C_i^*/C_a^*$ the quadrupole interaction predicts a jump in transition temperature, the smaller values for the packing fraction and $\Gamma$ but higher values of $C_i^*/k$, $\Delta\eta/\eta$, $S$, $\Delta\Sigma/Nk$ and $(dT_c/dp)_{p=1 \text{ bar}}$ in comparison with the anisotropic dispersion interaction, i.e. the discontinuity in the transition quantities increases due to quadrupole interaction.

Figure 9 shows the temperature dependence of the order parameter $S$ at constant pressure ($p = 1$ bar). The experimental values for the first two members of the homologous series of di-alkoxyazoxy-benzenes (PAA and PAP) are also plotted. The theoretical curves as obtained here as well as in I are given for $x = 1.0$ and 1.5. For a given value of $C_a^*/C_i^* = 1/12$ while the curve for $x = 1.0$ is close to the experimental values of PAA, the $x = 1.5$ curve is close to PAP.

TABLE III

The NI transition parameters in the present model system Eq. (8) and in the first two members of the homologous series di-alkoxyazoxybenzene (PAA and PAP), $S_c$ is the order parameter; $\bar{\eta} = (1/2)(\eta + \eta_i)$; $\eta$ and $\eta_i$ are nematic and isotropic packing fractions; $\Delta\Sigma/Nk$ the transition entropy; $\Gamma(T_c)$ is defined in Eq. (44). The model parameters are chosen so as to reproduce the transition temperature $T_c \simeq 409$ K.

| $x$ | $C_i^*/k$ | $C_i^*/C_a^*$ | $\bar{\eta}$ | $\frac{\Delta\eta}{\eta}$ | $S_c$ | $\frac{\Delta\Sigma}{Nk}$ | $\left(\frac{dT_c}{dp}\right)_{p=1\text{ bar}}$ | $\Gamma(T_c)$ |
|---|---|---|---|---|---|---|---|---|
| 1.0 | 4036.33 | 8 | 0.553 | 0.0168 | 0.473 | 0.829 | 61.58 | 1.42 |
| | 5273.30 | 12 | 0.608 | 0.0070 | 0.449 | 0.665 | 29.11 | 1.44 |
| 1.5 | 3051.35 | 8 | 0.469 | 0.0829 | 0.591 | 1.682 | 182.99 | 1.72 |
| | 3444.89 | 12 | 0.505 | 0.0440 | 0.537 | 1.209 | 122.84 | 1.83 |
| | 3941.36 | 20 | 0.540 | 0.0252 | 0.502 | 0.949 | 83.15 | 1.98 |
| | 4673.36 | 50 | 0.578 | 0.0145 | 0.478 | 0.779 | 54.30 | 2.23 |
| | 5027.54 | 100 | 0.593 | 0.0119 | 0.471 | 0.733 | 46.13 | 2.35 |
| 2.0 | 2664.76 | 12 | 0.4001 | 0.3030 | 0.741 | 3.852 | 398.18 | 2.19 |
| | 2819.45 | 20 | 0.429 | 0.1971 | 0.702 | 2.912 | 295.22 | 2.30 |
| | 3001.75 | 50 | 0.451 | 0.1357 | 0.662 | 2.297 | 235.45 | 2.45 |
| | 3074.66 | 100 | 0.459 | 0.1190 | 0.649 | 2.117 | 217.95 | 2.52 |
| PAA | | | 0.6189 | 0.0035 | 0.40<br>0.36 | 0.218 | 43.0 | 4.0 |
| PAP | | | 0.5179 | 0.0060 | 0.473<br>0.520 | 0.409 | | 2.5[a] |

[a] Taken from Tranfield and Collings.[15]

TABLE IV

Comparison of the NI transition parameters as obtained in I and the present work. The symbols have the same meanings as in Table III. The potential parameters are chosen so as to reproduce the transition temperature $T_c \simeq 409$ °K.

| $x$ | Pot. Model | $\frac{C_i^*}{K}$ | $\frac{C_i^*}{C_a^*}$ | $\bar{\eta}$ | $\frac{\Delta\eta}{\eta}$ | $S_c$ | $\frac{\Delta\Sigma}{Nk}$ | $\frac{dT_c}{dp}$ | $\Gamma(T_c)$ |
|---|---|---|---|---|---|---|---|---|---|
| 1.0 | Eq. (7) | 7321.74 | 12 | 0.663 | 0.0035 | 0.441 | 0.605 | 14.44 | 1.63 |
| | Eq. (8) | 5273.30 | 12 | 0.608 | 0.007 | 0.449 | 0.665 | 29.11 | 1.44 |
| 1.5 | Eq. (7) | 4311.41 | 20 | 0.561 | 0.0193 | 0.491 | 0.870 | 66.68 | 2.17 |
| | Eq. (8) | 3941.36 | 20 | 0.540 | 0.0252 | 0.502 | 0.949 | 83.15 | 1.98 |
| 2.0 | Eq. (7) | 2912.24 | 20 | 0.441 | 0.163 | 0.684 | 2.559 | 259.3 | 2.41 |
| | Eq. (8) | 2819.45 | 20 | 0.429 | 0.197 | 0.702 | 2.912 | 292.22 | 2.30 |

TABLE V

The NI transition parameters in the present model system Eq. (8) under high pressure

| $x$ | $C_i^*/k$ | $C_i^*/C_a$ | $P$ (bar) | $T$(°K) | $V^*$ | $\Delta V/V$ | $\frac{\Delta\Sigma}{Nk}$ | $S$ | $\frac{dT_c}{dP}$ | $\Gamma$ |
|---|---|---|---|---|---|---|---|---|---|---|
| 1.0 | 4036.3269 | 8 | 10 | 409.55 | 0.938 | 0.0165 | 0.824 | 0.470 | 60.99 | 1.424 |
| | | | 100 | 414.87 | 0.931 | 0.0146 | 0.788 | 0.468 | 55.77 | 1.426 |
| | | | 200 | 420.30 | 0.924 | 0.0129 | 0.756 | 0.464 | 51.03 | 1.428 |
| | | | 300 | 425.25 | 0.916 | 0.01167 | 0.738 | 0.461 | 47.85 | 1.430 |
| | 4273.2971 | 12 | 10 | 409.25 | 0.857 | 0.0069 | 0.663 | 0.449 | 28.97 | 1.444 |
| | | | 100 | 411.84 | 0.854 | 0.0066 | 0.653 | 0.448 | 27.58 | 1.448 |
| | | | 200 | 414.56 | 0.850 | 0.0062 | 0.644 | 0.447 | 26.20 | 1.445 |
| | | | 300 | 417.52 | 0.846 | 0.0058 | 0.633 | 0.446 | 25.36 | 1.445 |
| 1.5 | 3051.3507 | 8 | 10 | 410.70 | 1.069 | 0.0795 | 1.636 | 0.5869 | 179.72 | 1.72 |
| | | | 100 | 425.83 | 1.061 | 0.0568 | 1.325 | 0.5561 | 153.71 | 1.74 |
| | | | 200 | 440.34 | 1.050 | 0.0433 | 1.333 | 0.5341 | 133.53 | 1.76 |
| | | | 300 | 453.09 | 1.038 | 0.0352 | 1.0154 | 0.5193 | 118.76 | 1.78 |
| | 3444.8962 | 12 | 10 | 410.13 | 1.013 | 0.0429 | 1.19 | 0.5348 | 121.33 | 1.84 |
| | | | 100 | 420.59 | 1.004 | 0.0347 | 1.06 | 0.5198 | 108.65 | 1.86 |
| | | | 200 | 431.02 | 0.995 | 0.0288 | 0.964 | 0.5081 | 97.69 | 1.88 |
| | | | 300 | 440.50 | 0.985 | 0.0485 | 0.846 | 0.499 | 89.19 | 1.90 |
| 30AB[a] | | | 117.2 | 402.2 | 0.9213 | 0.0029 | | | | |
| | | | 189.0 | 405.2 | 0.9185 | 0.0020 | | | | |
| | | | 258.6 | 408.1 | 0.9153 | 0.0017 | | | | |

[a] The third member of the di-alkoxyazoxybenzene homologous series.[15]

### 3.2. Pressure induced phase transition properties

A study of the pressure induced mesomorphism is of particular importance. The higher pressure measurements in liquid crystals at constant molar volume show that the range of the stability of the liquid crystalline phase is increased considerably. McColl and Shih[13] were the first to report constant density measurement of order parameter $S$ in PAA. Their observed values of the temperature and pressure for NI transition are, respectively, 437.5°K and 640 bar. There are also known compounds[14] which at atmospheric pressure do not form liquid crystals but as the pressure is raised they exhibit mesophases. In addition, the measurements of thermodynamic properties under high pressure enable us to test the theories of the liquid crystalline state.

Very recently, Tranfield and Collings[15] have reported thermodynamic measurements under pressure for the first six members of the homologous series of di-alkoxyazoxybenzenes. They have measured

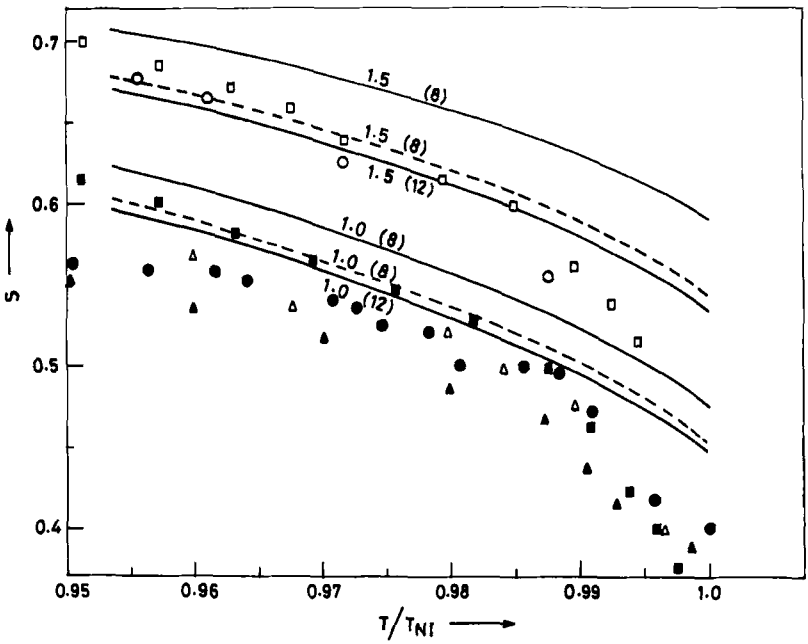


FIGURE 9 The temperature variation of the long-range orientational order parameter $S$ at constant pressure in PAA and PAP. $C_i^*/k$ are chosen so as to reproduce the nematic–isotropic transition temperature, $T_c = 409$ (°K). The experimental points are the observed values of Rowell *et al.*[16]—Ortho proton–proton splitting (● PAA, ○ PAP); Pines and Change[17]—para carbon-13 Chemzol shift (■ PAA, □ PAP) and de Jen and Classen[18]—magnetic susceptibility (▲ PAA, △ PAP). The number on the lines indicates value of $x$ and number in small bracket indicates the value of $C_i^*/C_a^*$. The line symbols are the same as in Figure 5.

the thermodynamic quantities throughout the nematic phase at constant volume as well as at constant temperature near the NI phase transition. From the measured data the role of end chain flexibility in a specific molecular geometry was investigated.

In this section, for the potential model of Eq. (8) we report the calculation for the pressure dependence of thermodynamic parameters for the NI transition. The temperature dependence of the order-parameter $S$ at constant density is shown in Figure 10. The experimental values for PAA and PAP are also given. The calculated values are obtained by starting at atmospheric pressure ($p = 1$ bar) and a temperature of about 390°K, the temperature is raised while keeping the density fixed as in the experiment of McColl and Shih.[13] The calculated values of temperature and pressure for NI transition are, respectively, 432.6°K and 420.1 bar for $x = 1.0$, $C_a/C_i^* = 1/8$;

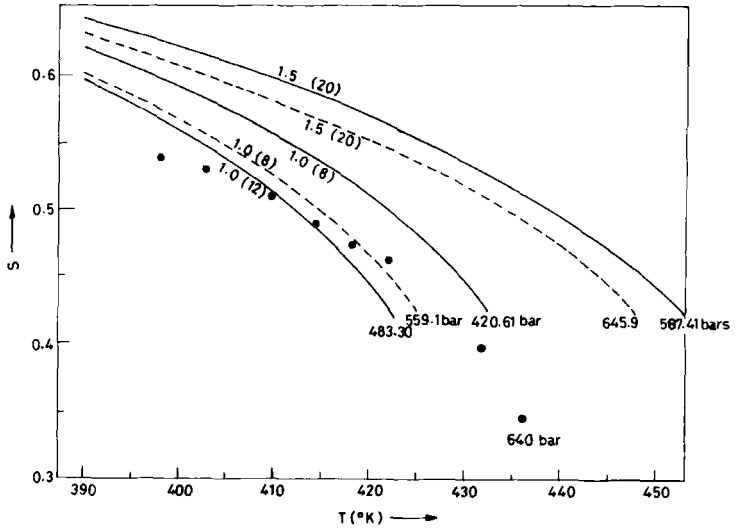


FIGURE 10 The temperature variation of long range orientational order parameter $S$ at constant density. The line symbols are the same as that of Figure 9. The numbers on the curves with and without small bracket indicate the values of $C_i^*/C_a^*$ and the values of $x$, respectively. The experimental points are those of McColl and Shih[13] from NMR measurements.

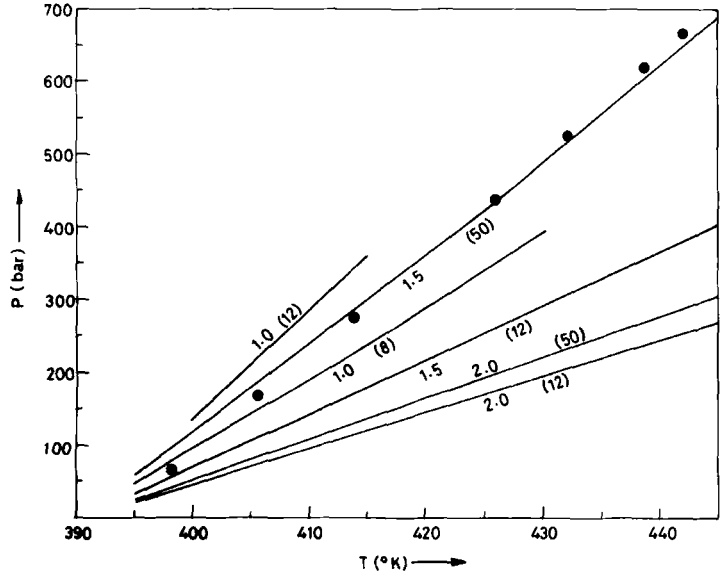


FIGURE 11 The variation of pressure with temperature for different values of $x$ and $C_i^*/C_a^*$ at constant density. The number in the small bracket indicates the value of $C_i^*/C_a^*$ and the number on the curves indicates the value of $x$. Experimental points for PAA are taken from Ref. 15.

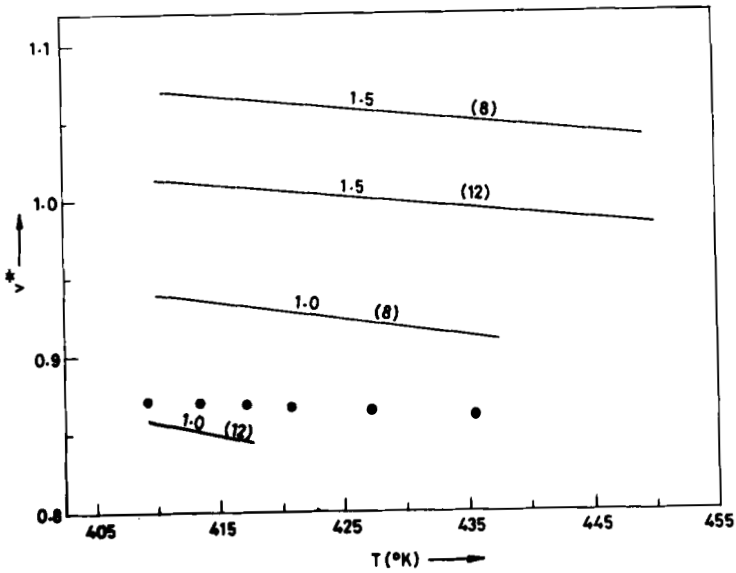


FIGURE 12 The temperature dependence of transition volume with pressure. The numbers with and without small bracket indicate values of $C_i^*/C_a^*$ and $x$, respectively. Experimental points are taken from Ref. 15.

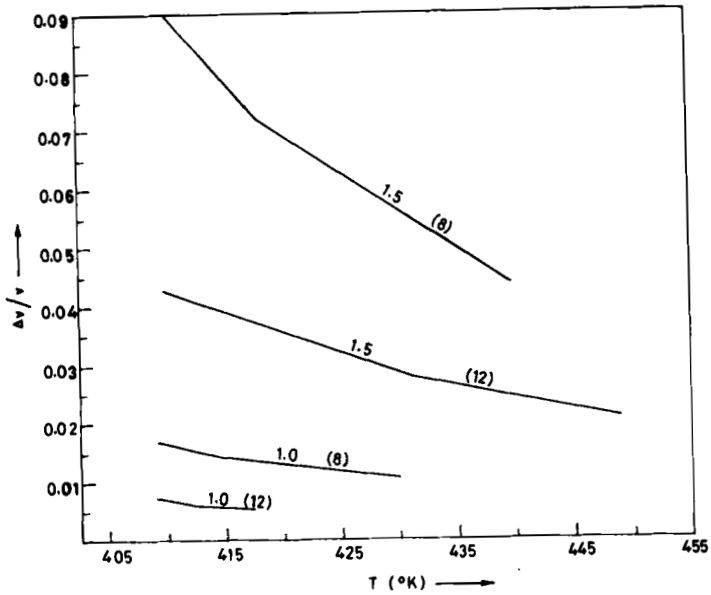


FIGURE 13 The temperature variation of the change in fractional volume with pressure. The numbers with and without small bracket indicate the values of $C_i^*/C_a^*$ and $x$, respectively.

422.7°K and 483.3 bar for $x = 1.0$, $C_a^*/C_i^* = 1/12$ and 452°K and 587.4 bar for $x = 1.5$ and $C_a^*/C_i^* = 1/20$.

Figure 11 is a plot of the variation of pressure with temperature for different values of $x$ and $C_i^*/C_a^*$. Experimental[15] values for PAA are also given. It is clearly seen from Figures 10 and 11 that the predicted values are in accordance with the values observed experimentally and the range of nematic phase is considerably larger at constant density as compared to its stability range at constant pressure.

The thermodynamic parameters at the NI phase transition are determined from Eq. (43) at various constant values of pressure ranging from 1 bar to 500 bar. The results are given in Table V. The temperature dependence of the transition volume is shown in Figure 12 whereas Figure 13 is a plot of fractional change in volume with temperature. Experimental values for PAA are also given in Figure 12. From these figures and the table several general trends are evident about the variation of NI transition properties with pressure: (i) As pressure increases the phase transition shifts to higher temperature and both the volume and the fractional volume change decrease. A decrease in the values of transition entropy, order parameter and $dT_c/dp$ is found whereas the parameter $\Gamma$ increases slightly. (ii) At a given pressure with the decreasing values of the ratio $C_a^*/C_i^*$ the values of the transition temperature, volume, fractional volume change, transition entropy, order parameter and $dT_c/dp$ decrease and the parameter $\Gamma$ increases. As shown in the table these predictions are in qualitative agreement of the observed[15] result. Quantitative agreement between the theory and experiment cannot really be expected but the results of the simple approach developed in this paper as well as in I is hoped to provide a basis for the interpretation of the thermodynamics of nematic liquid crystals.

## Acknowledgments

The authors are grateful to Dr. Y. Singh for helpful discussions and comments. KS wishes to thank Dr. P. P. Singh (Principal, M.L.K.P.G. College, Balrampur, India) for his interest and support and acknowledges the financial support of University Grants Commission (India) through the award of a Teacher Fellowship.

## References

1. M. A. Cotter, *J. Chem. Phys.*, **66**, 1098 (1977).
2. W. M. Gelbert and B. A. Baron, *J. Chem. Phys.*, **66**, 207 (1977).

3. J. G. J. Ypma and G. Vertogen, *Phys. Rev.*, **A17**, 1490 (1978).
4. V. T. Rajan and C. W. Woo, *Phys. Rev.*, **A17**, 382 (1978).
   L. Senbetu and C. W. Woo, *Phys. Rev.*, **A17**, 1529 (1978).
5. S. Singh and Y. Singh, *Mol. Cryst. Liq. Cryst.*, **87**, 211 (1982); In the text is referred to as I.
6. A. J. Leadbetter, R. M. Richardson and C. N. Colling, *J. de Phys.*, **36**, C1-37 (1975).
7. J. E. Lydon and C. J. Coakley, *J. de Phys.*, **36**, C1-45 (1975).
8. N. V. Madhusudana and S. Chandrasekhar, *Pramana, Suppl.*, **1**, 57 (1975).
9. W. Maier and G. Meier, *Z. Naturforschg.*, **16a**, 262 (1961).
10. J. D. Parson, *Phys. Rev.*, **19A**, 1225 (1979).
11. B. J. Berne and P. Puchukas, *J. Chem. Phys.*, **56**, 4213 (1972).
12. B. Larsen, J. C. Rasaiah and G. Stell, *Molec. Phys.*, **33**, 987 (1977).
13. J. R. McColl and C. S. Shih, *Phys. Rev. Lett.*, **29**, 85 (1972).
14. S. Chandrasekhar, *Liquid Crystals*, (Cambridge Univ. Press) Chapter 2 (1977).
15. R. V. Tranfield and P. J. Collings, *Phys. Rev.*, **A25**, 2744 (1982).
16. J. C. Rowell, W. D. Philips, L. R. Melby and M. Panar, *J. Chem. Phys.*, **43**, 3442 (1965).
17. A. Pines and J. J. Chang, *J. Am. Chem. Soc.*, **96**, 5590 (1974).
18. W. H. de Jeu and W. A. P. Classen, *J. Chem. Phys.*, **68**, 102 (1978).